ISSN 1808-8546 (ONLINE) 1808-3765 (CD-ROM)

PARÂMETROS BIOFÍSICOS ESTIMADOS PELO ALGORITMO METRIC EM ÁREA DE CULTIVADA NO SEMIÁRIDO DO ESTADO DO CEARÁ[1]

RENATA RICHELLE SANTOS DINIZ[2]; MAILSON ARAÚJO CORDÃO[3] E HUGO ORLANDO CARVALLO GUERRA[4]

[1] Trabalho oriundo da Dissertação de Mestrado do primeiro autor.
[2] Engenheira de Biossistemas, Discente do Curso de Doutorado do Programa de Pós-Graduação em Engenharia Agrícola, Universidade Federal de Campina Grande, Rua: Aprígio Veloso, 882, Bairro Universitário, Bodocongó, CEP: 58429-900. Campina Grande, Paraíba, Brasil. renata_richelle@hotmail.com.
[3] Engenheiro Agrônomo, Doutor em Engenharia Agrícola, Universidade Federal de Campina Grande, Rua: Aprígio Veloso, 882, Bairro Universitário, Bodocongó, CEP: 58429-900. Campina Grande, Paraíba, Brasil.. mailson.cordao@gmail.com.
[4] Engenheiro Agrônomo Ph.D. Professor Titular, Unidade Acadêmica de Engenharia Agrícola, Universidade Federal de Campina Grande, Rua: Aprígio Veloso, 882, Bairro Universitário, Bodocongó, CEP: 58429-900, Campina Grande, Paraíba, Brasil, hugo_carvallo@hotmail.com.

1 RESUMO

Análises espaciais e temporais de parâmetros biofísicos permitem avaliar no meio ambiente os impactos e as degradações decorrentes do uso e ocupação do solo, permitindo orientar políticas de reversão em um quadro de degradação ambiental. Dessa forma, o presente trabalho teve como objetivo estimar e analisar a dinâmica espaço–temporal dos parâmetros de albedo da superfície, NDVI e do IAF, através da aplicação do algoritmo METRIC (Mapping evapotranspiration at high resolution with internalized calibration) a partir de técnicas de sensoriamento remoto, em uma área irrigada com banana-nanica no município de Barbalha, CE. Na obtenção de tais estimativas foram utilizadas imagens do satélite Landsat-8 OLI/TIRS e dados meteorológicos da estação meteorológica automática localizada no município estudado em diferentes épocas do ano de 2016. Os resultados obtidos revelaram consistências com dados da literatura, que não houve grande variação temporal na área estudada para os parâmetros avaliados e que as temperaturas mais altas, foram estimadas em áreas de menores umidades. Conclui–se que os parâmetros biofísicos avaliados pelo algoritmo METRIC são eficazes e eficientes na compreensão da dinâmica dos padrões espaciais, temporais e espectrais de regiões semiáridas.

Keywords: sensoriamento remoto, NDVI, temperatura da superfície, TM-Landsat 8.

DINIZ, R. R. S.; CORDÃO, M. A. C.; GUERRA, H. O.C. BIOPHYSICAL PARAMETERS ESTIMATED BY THE METRIC ALGORITHM IN A CULTIVATED AREA IN THE SEMI-ARID OF THE STATE OF CEARÁ

2 ABSTRACT

Spatial and temporal analyses of biophysical parameters make it possible to assess the impacts and degradation resulting from land use and occupation on the environment, allowing guidance on reversal policies in the context of environmental degradation. Thus, the present

Recebido em 20/04/2022 e aprovado para publicação em 09/10/2023
DOI: http://dx.doi.org/10.15809/irriga.2023v28n4p791-804

work aimed to estimate and analyze the spatiotemporal dynamics of surface albedo parameters, NDVI, LAI and surface temperature through the application of the METRIC algorithm (mapping evapotranspiration at high resolution with internalized calibration) to remote sensing techniques in an irrigated area with a midget banana in the municipality of Barbalha, CE. To obtain such estimates, images from the Landsat-8 OLI/TIRS satellite and meteorological data from the automatic meteorological station located in the municipality studied at different times of the year 2016 were used. time in the study area for the evaluated parameters, and the highest temperatures were estimated in areas with lower humidities. The biophysical parameters evaluated by the METRIC algorithm are effective and efficient in understanding the dynamics of the spatial, temporal and spectral patterns of semiarid regions.

Keywords: remote sensing; NDVI, surface temperature, TM Landsat 8.

3 INTRODUCTION

The study of the variables that make up the energy balance, as well as values derived from heat flux and evapotranspiration, is essential for understanding the dynamics of the hydrological cycle. These estimates make it possible, for example, to plan irrigation activities, estimate the need for soil water replenishment and develop studies on subsurface water recharge, in addition to enabling the understanding of climate and environmental changes (Martins; Galvani, 2020).

Remote sensing-based solutions have been developed to minimize inconsistencies in methods related to measurements and information on consumptive water use, both at the agricultural crop scale and over large areas (watersheds to large geographic regions). However, existing methods lack validation, calibration and improvements that reflect the climatic and hydrological reality of the application area and that allow for more accurate ET estimates (Melton *et al*.). , 2022).

The use of space science techniques such as remote sensing and satellite technology for ET estimation in agriculture has recently become very popular. This approach provides a consistent and cost-effective solution to field-based measurement methods. Typically, sensors in the field provide input recommendations and regulate water and nutrient requirements. The spatial variation in these requirements is captured by GPS receivers (Djaman *et al*., 2018). Therefore, Liakos *et al.* (2018) reported that automated area management using agricultural automation equipment and systems will be increasingly widely used in the future. Deep learning technology and spectral analysis can be used as examples.

In recent decades, production systems have improved techniques for producing more water, reducing the volume of water applied, especially in regions such as the Brazilian semiarid region, which faces the problem of water scarcity (Santiago *et al.*, 2017; Oliveira; Braga, 2019; Silva; Barbosa, 2021).

The determination of biophysical parameters by sensing techniques has several purposes, which generally involve estimating the change in vegetation cover over time caused by human activity in the area of interest, as seen in the studies by Simões, Lima and Mendonça (2021), Ivo *et al.* (2020), Leal *et al.* (2019), Silva *et al.* (2019) and Pezzoni Filho *et al.* (2018).

According to Diniz *et al.* (2021), the use of remote monitoring allows estimation, in addition to the components of the water balance, of the actual daily evapotranspiration via the METRIC algorithm, obtaining results in line with those found in the bibliography, for the irrigated area.

The use of biophysical parameters used in environmental monitoring, some of which are used to determine energy balance and evapotranspiration, makes it possible to more easily estimate desertification processes, indicating possible terrestrial degradation, as advocated by Allen *et al.* (2002), who state that it encourages the use of techniques such as remote sensing, which allows the use of reliable and more precise methods through satellite images.

The determination of biophysical parameters by sensing techniques has several purposes: measuring the variability in vegetation cover, assessing environmental impacts and quantifying anthropogenic interference in different classes of land use. In addition, they are used in the process of determining the actual evapotranspiration of irrigated crops (Cordão *et al*.). 2023).

The determination of biophysical parameters such as albedo, the normalized difference vegetation index and surface temperature by sensing techniques has several purposes, which, in general, is to estimate the change in vegetation cover over time caused by human activity in the study area, as verified by Simões, Lima and Mendonça (2021) and Ivo *et al.* (2020).

Among the various biophysical indices most commonly used, albedo, which is found on vegetated surfaces, depends on the texture of the soil and the physiological conditions of the plant canopy. In dry soil, the albedo is significantly greater than that observed in moist soil, whereas a smooth surface has a greater albedo than a rough surface (Martins; Rosa, 2016).

The normalized difference vegetation index (NDVI) is one of the most widely used vegetation indices in remote sensing. It is calculated from red and near-infrared reflectances and excels in identifying vegetated areas with greater precision (Santana *et al*., 2018). The NDVI has been used to express vegetation variability, observe its correlation with climatic conditions (Chu *et al*., 2019), assess vegetation in precision agriculture, and monitor plant health and crop growth status (Nicholas; Ng; Tew, 2022; Bouskour; Bahatti; Zaggaf, 2023).

According to Ruhoff (2011), surface temperature (Ts) is very important for describing Earth's surface processes and is used in climatic, hydrological, and biological studies. Therefore, there are significant correlations between surface temperature and most variables, indicating that surface temperature is the main biophysical parameter for determining radiation balance, heat fluxes and evapotranspiration (Martins; Galvani, 2020). Given the above, the objective of this study is to perform a spatiotemporal analysis of the vegetation area in a municipality in the Brazilian semiarid northeastern region via biophysical indices, albedo, the normalized difference vegetation index (NDVI), and the leaf area index (LAI).

4 MATERIALS AND METHODS

4.1. Characterization of the study area

The study was carried out in an area where dwarf bananas (*Musa* spp.) are cultivated, which is located in the municipality of Barbalha (Figure 1), in the Cariri Metropolitan Region of the state of Ceará, whose geographic coordinates are 07° 17' 07.91" South and 39° 12' 58" West (Google Earth Pro, 2020).

The city of Barbalha is 553 km from the state capital, with an altitude of 415 m above sea level; has an area of 569.51 km²; has a population of 55,533 inhabitants; is located at the foot of Chapada do Araripe;

and has a GDP equivalent to R$ 455,763.00 (IBGE, 2015).

Figure 1. Location of the experimental area in Barbalha, CE

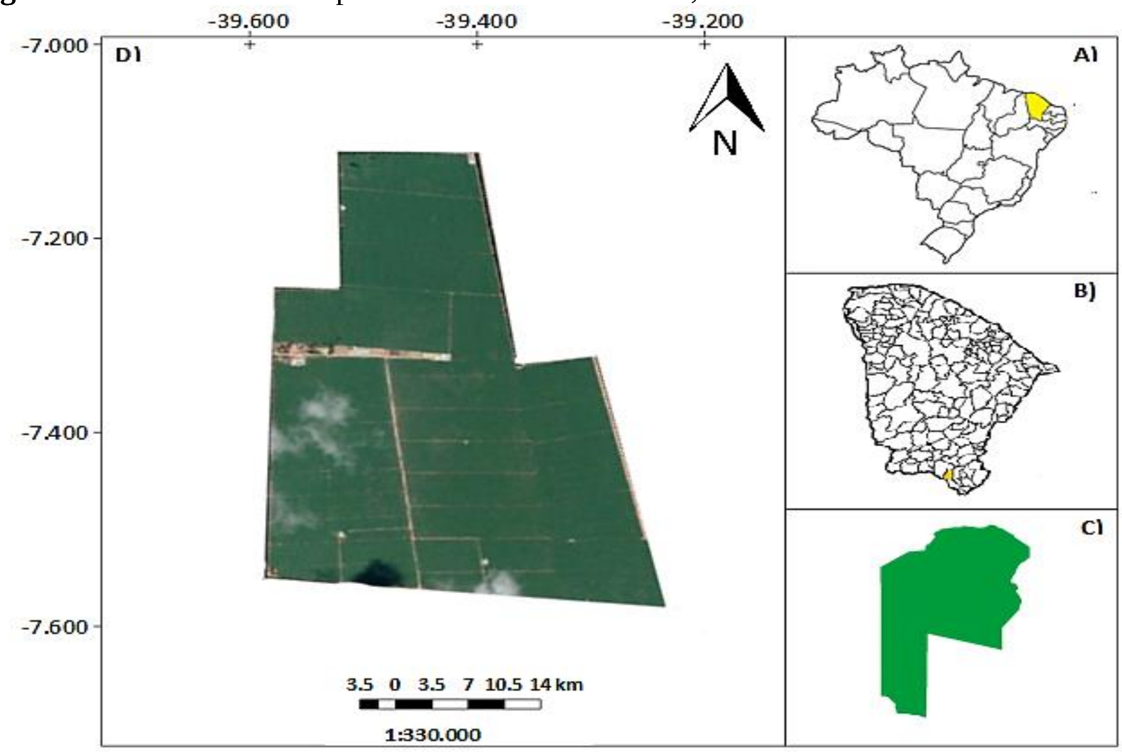

Highlighting the sample plot with irrigated cultivation of dwarf banana [D]- In [A], the map of Brazil highlights the State of Ceará; in [B], the map of Ceará highlights the Metropolitan Region of Cariri; and in [C], the map of the municipality of Barbalha, 2024.
Source: The authors (2024)

4.2. Data

The climate information collected was obtained from the automatic meteorological station in Barbalha, Ceará (National Institute of Meteorology, 2016).

The Operational Land Imager (OLI) and Thermal software were used. The infrared sensor - TIRS of the Landsat 8 satellite, orbit 217 and point 65, acquired from the United States Geological Survey (USGS, 2016), corresponds to the following days: May 22 (days after sowing (DAS) 143), August 10 (DAS 223), and October 29 (DAS 303) of 2016.

4.3. Methodological procedures

After the images were obtained from the USGS, ERDAS Imagine software was used. This model allows the graphic creation of a workflow and execution from one or more input data points, producing an output (aster image). It is used to perform the processes of stacking the bands, cropping the stacked images, and processing the images via the Model Maker tool, which is responsible for mathematical operations for each stage assigned to the study and is an indispensable tool for processing the images and obtaining estimates of the radiation and energy balances.

The computational steps in the process of obtaining biophysical parameters through METRIC are described in the diagram represented in Figure 2.

Figure 2. Diagram of computational steps in processing to obtain biophysical parameters via the METRIC algorithm.

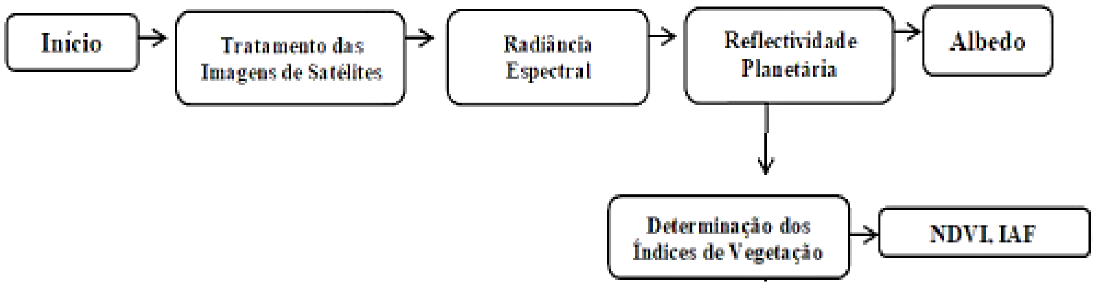

Source: The authors (2024)

The computational steps described above began with the selection and processing of images that occurred according to the choice of images with low cloud cover, aiming at better processing quality, meeting the research requirements and the dates with the representation of the soil cover conditions in rainy and dry periods. Using the data obtained from the meteorological station described in Table 1, it was possible through METRIC to estimate the biophysical parameters as described below.

Table 1. Meteorological data used to obtain the reference evapotranspiration (ET_{θ}) according to the Penman–Monteith method for the Barbalha-CE region.

Date of images	Temperature (°C)		U. relative (%)		Speed Wind, (m/s)	Radiation Global MJ/m2 / d	ET_r of Reference (mm)
	Max	Min	Max	Min			
05/22/2016	28.4	26.7	75.0	71.0	2.1	22.9	4.1
10/08/2016	23.3	19.6	69.0	63.3	2.2	23.5	4.5
10/29/2016	24.8	21.0	57.6	51.3	2.1	27.9	5.9

U: Humidity; Max: Maximum; Min: Minimum
Source: DINIZ *et al.* (2021)

METRIC was used to estimate the different components of the surface energy balance. The first step, called spectral radiance or radiometric calibration (Lb), corresponds to the solar energy reflected by each pixel per unit of area, time, solid angle and wavelength measured at the Landsat 8 OLI/TIRS satellite level for bands 2, 3, 4, 5, 6 and 7 and thermal band 10. It is determined on the basis of the additive and multiplicative terms in each band via Equation 1 (Chander; Markham, 2003; Silva *et al.*, 2016).

$$L_b = Add_{rad,b} + Mult_{rad,b} . ND_b \qquad (1)$$

Where $Add_{rad,b}$ is the additive term and $Mult_{rad,b}$ is multiplicative relative to the radiance (extracted from the metadata of each OLI image) and is the intensity of each pixel and the band (values between 0 and 65,365) observed from the images.

To determine the planetary reflectivity (r_b), it was necessary to convert the quantized and calibrated gray level values of each OLI band to reflectances. In this way, the radiometric coefficients related to reflectance, available in the image metadata, were used (Chander; Markham, 2003; Silva *et al.*, 2016). The monochromatic reflectance of each pixel r_b(W m $^{-2}$ sr $^{-1}$ μm $^{-1}$) is given by Equation 2:

$$r_b = \frac{(Add_{ref,b} + Mult_{ref,b}.ND_b)}{\cos Z.d_r} \quad (2)$$

4.3.1. Surface albedo

It is given by the ratio of the reflected solar radiation to the global solar radiation incident on the surface in the entire domain of shortwave radiation at the surface (0.3--3.2 μm). The computation of α_s is obtained through Equation 3 with the linear combination of the monochromatic reflectances of each band:

$$\alpha_s = \sum_{b=1}^{n}(\rho_{s,b} \cdot \omega_b) \quad (3)$$

Where ω_b expresses the weight of each band, $\rho_{s,b}$ represents the reflectance of each TM band, and the reflectance of each band corrected for atmospheric effects is given by the ratio between the reflected solar radiation - $R_{out\ s,b}$ for each band and the incident radiation- $R_{in\ s,b}$ (Equation (4)) on the surface, which can be expressed according to the following expression (Allen; Tasumi; Trezza, 2007):

$$\rho_{s,b} = \frac{R_{out\ s,b}}{R_{in\ s,b}} = \frac{\rho_{t,b} - \rho_{a,b}}{\tau_{in,b} \cdot \tau_{out,b}} \quad (4)$$

Where $\rho_{s,b}$ is the reflectivity of the pixel to the surface; $\rho_{t,b}$ is the b-band reflectivity at the top of the atmosphere; $\rho_{a,b}$ is the atmospheric reflectance; $\tau_{in,b}$ is the atmospheric transmissivity for incident solar radiation; and $\tau_{out,b}$ is the transmissivity for solar radiation reflected by the surface. According to Allen, Tasumi and Trezza (2007), $\tau_{in,\ b}$, and $\tau_{out,\ b}$ are responsible for the attenuation of both beams and diffuse radiation.

The b-band reflectivity at the top of the atmosphere is estimated according to Equation 5 (Allen; Tasumi; Trezza, 2007):

$$\rho_{t,b} = \frac{\pi L_{t,b} d^2}{ESUN_b \cos\theta_{rel}} \quad (5)$$

where $L_{t,b}$ = the reflected energy measured in the b-band from the satellite (Wm $^{-2}$ ster $^{-1}$ μ $^{m-1}$), d = the Earth–Sun distance in astronomical units, $ESUN_b$ is the mean solar exoatmospheric radiation over the b-band (Wm $^{-2}$ μm $^{-1}$), and cos θ_{rel} is the cosine of the solar angle of incidence (or solar zenith angle) relative to the normal to the inclination of the Earth's surface and can be determined via Equation 6 (Allen; Tasumi; Trezza, 2007):

$$\cos(\theta) = \sin(\delta)\sin(\phi)\cos(S) - \sin(\delta)\cos(\phi)\sin(S)\cos(\gamma) \quad (6)$$

Where δ is the sun's declination, ϕ is the central latitude of the scene, s is the pixel tilt (s = 0 for horizontal slope and $s=\frac{\pi}{2}$ for vertical slope), ω is the hour angle in radians (ω = 0 at noon, negative in the morning and positive in the afternoon), and γ is the azimuthal angle of the surface (γ = 0 for south-facing slopes, γ = $-\frac{\pi}{2}$for east-facing slopes, γ = $+\frac{\pi}{2}$ for west-facing slopes and γ = $\pm\pi$ for north-oriented slopes). The atmospheric reflectance $\rho_{a,b}$ is given by Equation 7 (Allen; Tasumi; Trezza, 2007):

$$\rho_{a,b} = C_b(1 - \tau_{in,b}) \quad (7)$$

where C_b is the coefficient derived from the radiative transfer model. The transmittance values are given according to Allen, Tasumi and Trezza (2007) and are determined via Equations 8 and 9:

$$\tau_{\text{in,b}} = C_1 exp\left[\frac{C_2 P}{K_1 \cos\theta_{hor}} - \frac{C_3 W + C_4}{\cos\theta_{hor}}\right] + C_5 \quad (8)$$

$$\tau_{\text{out,b}} = C_1 exp\left[\frac{C_2 P}{K_1 \cos ŋ} - \frac{C_3 W + C_4}{\cos ŋ}\right] + C_5 \quad (9)$$

Where C1, C2, C3, C4 and C5 are the coefficients derived from the radiative transfer model, which are the same as those indicated by Allen, Tasumi and Trezza (2007); P is the atmospheric pressure (kPa); W is the precipitable water (mm); K_1 is the atmospheric turbidity coefficient (default value = 1.0); andθ_{hor} is the solar zenith angle, ŋ which is the angle of view of the sensor relative to the perpendicular horizontal surface. In the case of Landsat, the cosŋ $= 1$.

The value of $\cos\theta_{hor}$ is obtained by reducing Equation (6), giving rise to Equation (10).

$$\cos\theta_{hor} = \sin(\delta)\sin(\phi) + \cos(\delta)\cos(\phi)\cos(\omega) \quad (10)$$

4.3.2. Vegetation indices (NDVI, LAI)

The normalized difference vegetation index (NDVI) is a ratio of the difference in the reflectances of the near-infrared (ρ_{IV}) and red (ρ_V) bands to the sum of the same (Equation (11)) according to Allen *et al.* (2002), in which the corresponding bands in Landsat 8 are bands 4 and 5.

$$NDVI = \frac{(\rho_{IV} - \rho_V)}{(\rho_{IV} + \rho_V)} \quad (11)$$

The LAI-leaf area index is defined by the ratio between the leaf area of all vegetation per unit area used by this vegetation and is considered an indicator of the biomass of each pixel in the image (Allen *et al*., 2002). Its equation is based on the calculation involving SAVI, using Equation (12), obtained by Allen *et al.* (2002):

$$\text{IAF} = -\frac{\ln\left(\frac{0{,}69 - \text{SAVI}}{0{,}59}\right)}{0{,}91} \quad (12)$$

5 RESULTS AND DISCUSSION

5.1 Surface albedo

Figure 3 (A, B and C) shows thematic maps of the surface albedo in an experimental area in the municipality of Barbalha, CE. The cultivated area (highlighted by the black line) presented an albedo of 0.16 on May 22, 0.16 on August 10, and 0.18 on October 29. The highest albedo values obtained by METRIC in the area varied between 0.26 and 0.38 in places with exposed soil, and the lowest albedo values were between 0.09 and 0.14.

Figure 3. Thematic maps of surface albedo in the municipality of Barbalha, CE: May 22 (A), August 10 (B) and October 29 (C) of 2016.

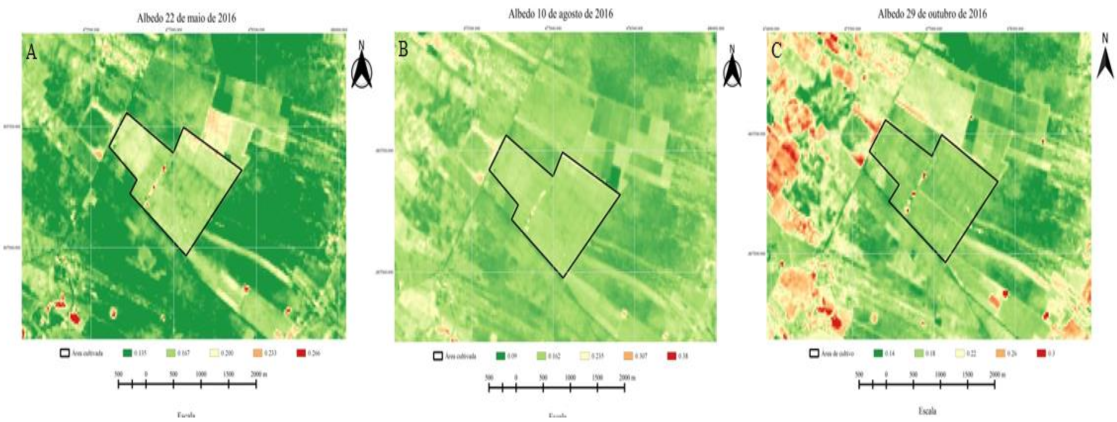

Source: The authors (2023)

In general, the surface albedo values did not vary significantly, but in October, which is the dry season in the region, a greater concentration of extreme surface albedo values was observed around the study area, confirming the estimate by Bezerra *et al.* (2014), who obtained higher albedo values during the dry season in areas of exposed soil in the semiarid region of the state of Rio Grande do Norte.

5.2 Vegetation Indices

5.2.1 NDVI

Figure 4 (D, E and F) shows thematic maps of the NDVI in an experimental area (highlighted by the black line) in the municipality of Barbalha, CE, with NDVI values of 0.85 on May 22, 0.83 on August 10 and October 29.

The lowest NDVI values were observed in areas with an exposed soil density of 0.26 and from 0.35 to 0.52 in areas with low vegetation density. These results corroborate the values reported by Santos *et al.* (2020), who reported the lowest NDVI values in exposed soil in the state of Alagoas in 2016. In addition, Alves *et al.* (2015) and Gomes *et al*. (2013) reported values between 0.09 and 0.25 for exposed soil in the municipality of Água Branca, AL, and in areas of sparse vegetation, values ranging from 0.26--0.43 were found.

Figure 4. NDVI thematic maps in the municipality of Barbalha, CE: May 22 (D), August 10 (E) and October 29 (F) of 2016.

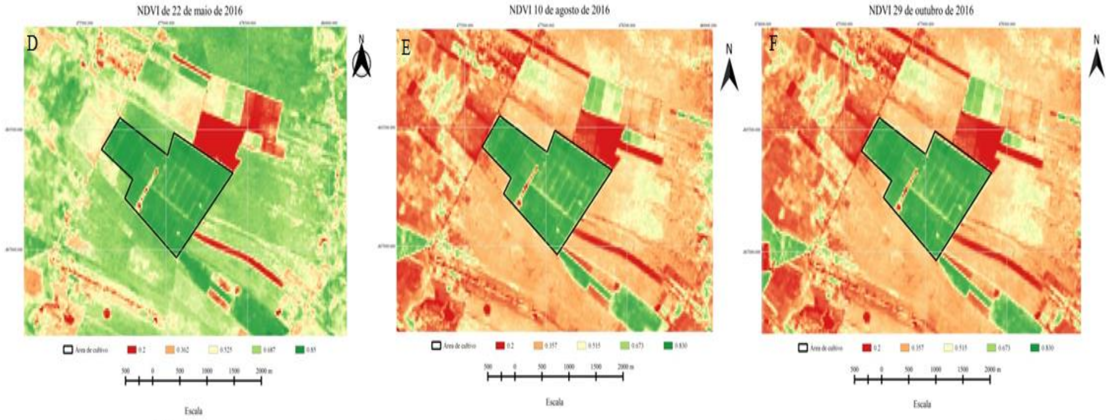

Source: The authors (2023)

5.2.2 IAF

Figure 5 (G, H and I) shows thematic maps of IAF-METRIC. The higher IAF values in the irrigated agricultural area, which ranged between 4.0 and 6.0, were considered high compared with those reported by Gameiro *et al*. (2016), who, in an area with natural irrigation of fruit growing, in the coastal region of Ceará, identified an IAF of 0.11 in a wet period, and by Oliveira *et al.* (2012), who obtained instantaneous average IAF results between 0.40 and 2.47.

Figure 5. Thematic charts of the leaf area index (IAF - METRIC) in the municipality of Barbalha - CE: May 22 (G), August 10 (H) and October 29 (I) of 2016**.**

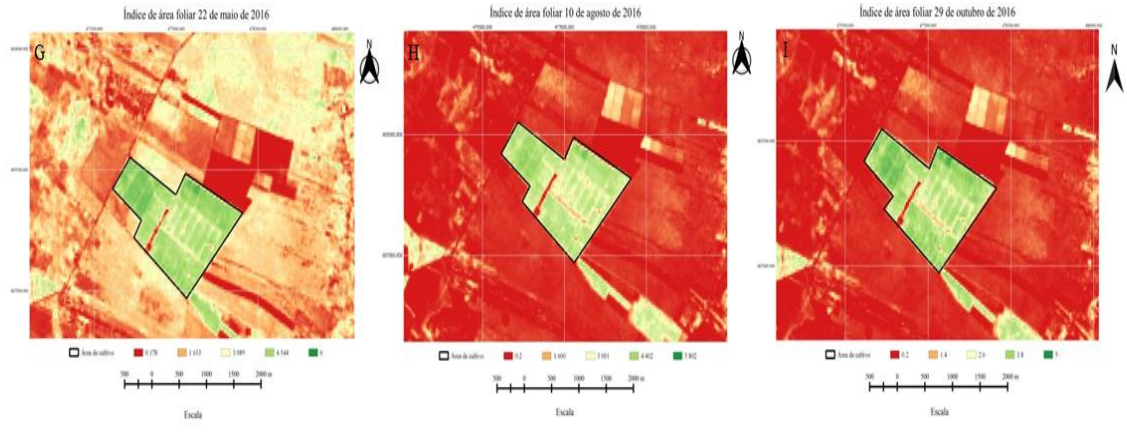

Source: The authors (2023)

6 CONCLUSION

Remote sensing techniques have made it possible to identify, map and analyze the biophysical parameters of the surface in an irrigated area in the State of Ceará.

There were no significant variations in surface albedo for the period studied.

The vegetation indices (NDVI and IAF) are related to rainfall; the month of May, which precedes the rainy season in the Ceará region, is the period that presents conditions for the development of banana crops, leading to the most expressive values of these indices.

Finally, research on this topic is relevant, as it analyzes physical–chemical interactions and interferences and, with the use of algorithms such as METRIC, allows the identification of differences in the spatial and temporal patterns of biophysical parameters in response to land use and occupation and generates support for adequate management and decision-making regarding water resources.

7 ACKNOWLEDGMENTS

The authors would like to thank the Coordination for the Improvement of Higher Education Personnel (CAPES) for the scholarships granted to the authors, enabling work and research such as this.

8 REFERENCES

ALLEN, RG; TASUMI, M.; TREZZA, R.; WATERS, R.; BASTIAANSSEN, W. **SEBAL** - Surface Energy Balance Algorithm for Land. Advanced training and User Manual. Version 1.0. Kimberly: University of Idaho, 2002.

ALLEN, RG; TASUMI, M.; TREZZA, R. Satellite-Based energy balance for mapping evapotraspiration with internalized calibration (METRIC) – Model. **Journal of Irrigation and Drainage Engineering** , Reston, vol. 133, no. 4, p. 380-394, 2007.

ALVES, LER; GOMES, HB; SILVA, EFS; SANTOS, MN; SANTOS, C.; CABRAL, SL Mapping of IVDN and IVAS for the municipality of Coqueiro Seco -AL from images generated by Thematic Landsat Mapper 5. *In* : SYMPOSIUM ON GEOTECHNOLOGIES AND GEOINFORMATION OF THE STATE OF ALAGOAS, 3., 2015, Maceió. **Proceedings** [...]. Alagoas : Geo Alagoas , 2015. p. 181-188. Available at: https://dados.al.gov.br/catalogo/es/dataset/anais-do-3-geoalagoas-simposio-sobre-as-geotecnologias-e-geoinformacao-no-estado-de-alagoas-2015/resource/5190fcd9-999f-4a52-8cfa-ead906cb2cfe. Accessed on: November 10, 2023.

BEZERRA, JM; MOURA, GBA; SILVA, BB; LOPES, PMO; SILVA, EFF Biophysical parameters obtained by remote sensing in semiarid region of Rio Grande do Norte state, Brazil. **Brazilian Journal of Agricultural and Environmental Engineering** , Campina Grande, v. 18, n.1, p. 73-84, 2014.

BOUSKOUR, S.; BAHATTI, L.; ZAGGAF, MH The use of NDVI to improve cereals agriculture : A review. *In:* INTERNATIONAL CONFERENCE ON INNOVATIVE RESEARCH IN APPLIED SCIENCE, ENGINEERING AND TECHNOLOGY, 3., 2023, Mohammedia . **Processing** [...]. Morocco : IEEE, 2023. p. 1-7. DOI: https://doi.org/10.1109/IRASET57153.2023.10153054. Available at: https://ieeexplore.ieee.org/document/10153054. Accessed: June 5, 2023.

CORDÃO, M. A; DINIZ, RR S; GUERRA, HO C; SANTOS, CL M; Actual evapotranspiration of the dwarf coconut tree determined by the METRIC model parameterized in the semiarid region of Paraíba. **Irriga** , Botucatu, v. 28 , n. 1, p. 134-147, 2023.

CHANDER, G.; MARKHAN, B. Revised Landsat 5 - TM radiometric calibration procedures and post calibration dynamic ranges. **IEEE Transactions on Geosciences and Remote Sensing** , New York , v. 41, no. 11, p. 2674-2677, 2003.

CHU, H.; VENEVSKY, S.; Wu, C.; WANG, M. NDVI- based vegetation dynamics and its response to climate changes at Amur- Heilongjiang River Basin from 1982 to 2015. **Science of the Total Environment** , Amsterdam, v. 650, p. 2051-2062, 2019. DOI: https://doi.org/10.1016/j.scitotenv.2018.09.115. Available at: https://www.sciencedirect.com/science/article/pii/S0048969718335575. Accessed on: June 7, 2022.

DJAMAN, K.; O'NEILL, M.; SMEAL, D.; KOUDAHE, K.; WEST, M.; LOMBARD, K.; IRMAK, S. Crop evapotranspiration, irrigation water requirement and water productivity of corn from meteorological data in a semiarid climate. **Water** , Basel, v. 10, n. 4, p. 405- 421, 2018.

DINIZ, RRS; CORDÃO, MAC; GUERRA, HOC; OLIVEIRA, CW Biophysical parameters estimated by the METRIC algorithm in cultivated areas in the semiarid region of Ceará state. **Irriga Magazine** , Botucatu, v. 26, n. 3, p. 701-716, 2021. DOI: https://doi.org/10.15809/irriga.2021v26n3p701-716. Available at: https://revistas.fca.unesp.br/index.php/irriga/article/view/4448. Accessed on: February 12, 2024.

GAMEIRO, S.; TEIXEIRA, CPB; SILVA NE TO, TA; L OP E S, MDL; DUARTE, CR; S OUTO, MVS; ZIMBACK, CR L . Assessment of vegetation cover using vegetation indices (NDVI, SAVI and IAF) in the Lower Jaguaribe Hydrographic Sub-Basin, CE. **Terræ** , Campinas, v. 13, n. 1/2., p. 15-22, 2016.

GOMES, HB; SILVA JUNIOR, RS; PACE, FT Thematic mapping of vegetation cover in the microregion of the São Francisco backlands of Alagoas, using TM LANDSAT 5 images. **Brazilian Journal of Physical Geography** , Recife, v. 5, n. 5, p. 1121-1132, 2013.

GOOGLE EARTH. **Google Earth Pro. version** 9.152.0.1. [*S. l.*]: Google, 2020. Available at: http://earth.google.com/. Accessed on: September 20, 2022.

IBGE. **Economic Profile and infographics of the city of Barbalha** . Rio de Janeiro: IBGE, 2015. Available at: https://bdiaweb.ibge.gov.br/#/consulta/pedologia. Accessed on: January 15, 2023.

NATIONAL INSTITUTE OF METEOROLOGY. **Annual historical data** . Brasília, DF: INMET, 2016. Available at: https://bdmep.inmet.gov.br/. Accessed on: September 18, 2020.

IVO, IO; BIUDES, MS; COSTA, RO; MACHADO, NG; SANTOS, L OF; PEDREIRA JUNIOR, AL Temporal variation of surface biophysical parameters by Landsat 5 images in different land covers in a transition area of Cerrado and Pantanal in Mato Grosso. **Nativa** , Sinop, v. 8, n. 5, p. 597-602, 2020. DOI: https://doi.org/10.31413/nativa.v8i5.10064. Available at: https://periodicoscientificos.ufmt.br/ojs/index.php/nativa/article/view/10064. Accessed on: September 18, 2022.

LEAL, FA; SOUZA, CM; LEAL, GSA; MIGUEL, EP Use of NDVI in the analysis of vegetation after fire occurrence. **Nativa** , Sinop, v. 7, n. 2, p. 226- 231, 2019. DOI: http://dx.doi.org/10.31413/nativa.v7i2.6664 . Available at https://periodicoscientificos.ufmt.br/ojs/index.php/nativa/article/view/6664. Accessed on: September 10, 2023.

LIAKOS, KG; BUSATO, P.; PEARSON, S.; BOCHTIS, D. Machine learning in agriculture: A review. **Sensors** , Basel, v. 18, n. 8, article 2674, p. 2674- 2703, 2018.

MARTINS, A.; GALVANI, E. Performance of the SEBAL algorithm for estimating flow in watersheds of the Brazilian Cerrado. **Sociedade & Natureza** , Uberlândia
v. 32. p. 687-698, 2020. DOI: https://doi.org/10.14393/SN-v32-2020-53169. Available at: https://seer.ufu.br/index.php/sociedadenatureza/article/view/53169/30030. Accessed on: July 6, 2023.

MARTINS, AP; ROSA, R. Surface albedo estimation using Modis/Aqua images and the SEBAL algorithm in the Paranaíba River Basin-Brazil. *In* : INTERNATIONAL SYMPOSIUM ON REMOTE PERCEPTION AND GEOGRAPHIC INFORMATION SYSTEMS , 17., 2016, Puerto Iguazú. **Proceedings** [...]. Puerto Iguazú: SELPER, 2016. p. 3045-3058.

MELTON, FS; HUNTINGTON, J.; GRIMM, R.; HERRING, J.; HALL, M.; ROLLISON, D.; ERICKSON, T.; ALLEN, R.; ANDERSON, M.; FISHER, JB; KILIC, A.; SENAY, GB; VOLK, J.; HAIN, C.; JOHNSON, L.; RUHOFF, A.; BLANKENAU, P.; BROMLEY, M.; CARRARA, W.; DAUDERT, B.; DOHERTY, C.; DUNKERLY, C.; FRIEDRICHS, M.; GUZMÁN, A.; HALVERSON, G.; HANSEN, J.; HARDING, J.; KANG, Y.; KETCHUM, D.; MINOR, B.; MORTON, C.; ORTEGA-SALAZAR, S.; OZDOGAN, TOM; REVELLE, PM; SCHULL, M.; WANG, C.; Yang, Y.; ANDERSON, RG Filling a critical data gap in water management for the western United States. **Journal of the American Water Resources Association** , Herndon , v. 58, n. 6, p. 971-994, 2022 . DOI: https://doi.org/10.1111/1752-1688.12956. Available at https://onlinelibrary.wiley.com/doi/epdf/10.1111/1752-1688.12956. Accessed on: June 2, 2023.

NICHOLAS, NJH; NG, YP; TEW, Y. Intelligent Farming with NDVI Integrated Agriculture Solution . *In* : INTERNATIONAL CONFERENCE ON GREEN ENERGY, COMPUTING AND SUSTAINABLE TECHNOLOGY, 2022 , Miri Sarawak. **Annals** [...]. Piscataway : IEEE, 2022. p. 342-345, 2022. DOI: https://doi.org/10.1109/GECOST55694.2022.10010427. Available at: https://ieeexplore.ieee.org/document/10010427. Accessed on: 17 Jan. 2021.

OLIVEIRA, AR; BRAGA, MB Sugarcane varieties subjected to different water replacement depths by subsurface drip. **Energy in Agriculture,** Botucatu, v. 32 , n. 3, p. 350-366, 2019. Available DOI: https://doi.org/10.17224/EnergAgric.2019v34n3p350-363. Available at: https://www.alice.cnptia.embrapa.br/alice/handle/doc/1120210 . Accessed on: February 8, 2021 .

OLIVEIRA, LMM; MONTENEGRO, SMGL; ANTONINO, ACD; SILVA, BB; MACHADO, CCC; GALVÍNCIO, JD Quantitative analysis of biophysical parameters of river basins obtained by remote sensing. **Brazilian Agricultural Research** , Brasília, DF, v. 47, n. 9, p. 1209-1217, 2012.

PEZZONI FILHO, JC; LESSA, LGF; FILGUEIRAS, R.; LEDA, VC; ZIMBACK, CRL; FURTADO, EL Leaf vigor behavior in rubber trees under different canopy phenologies. **Nativa** , Sinop, v. 6, n. 5, p. 497-506, 2018. DOI: http://dx.doi.org/10.31413/nativa.v6i5.5279 . Available at: https://periodicoscientificos.ufmt.br/ojs/index.php/nativa/article/view/5279. Accessed on: Apr. 12, 2022.

RUHOFF, AL **Remote sensing applied to the estimation of evapotranspiration in tropical biomes** . Thesis (PhD in Water Resources and Environmental Sanitation) – Universidade Federal do Rio Grande do Sul, Porto Alegre, 2011.

SANTANA, SHC; SILVA, ERAC; LAURENTINO, MLS; MELO, JGS; GALVÍNCIO, JD Identification of vegetation indices with the best spectral responses for the Atlantic Forest in the city of São Paulo-SP. **Journal of Environmental Analysis and Progress** , Recife, v. 3, n. 2, p. 200-209, 2018. DOI: https://doi.org/10.24221/jeap.3.2.2018.1765.200-209. Available at https://www.journals.ufrpe.br/index.php/JEAP/article/view/1765. Accessed on: April 10, 2022.

SANTIAGO, AD; CHICO, D.; ANDRADE JUNIOR, AS; GARRIDO, A.; CARNAÚBA, PJP Water footprint of sugarcane and ethanol produced in the state of Alagoas, Brazil. **Agrometeoros** , Mossoró, v. 25 , n. 1, p. 209-216, 2017.

SANTOS, FS; GOMES, HB; BARROS, GVP; ALVES, LER; SILVA, DF; COSTA, RL; SILVA, FDS; OLIVEIRA JUNIOR, JF Seasonal Analysis of Biophysical Parameters Using the MODIS Sensor for the State of Alagoas . **Brazilian Journal of Meteorology** , São José dos Campos, v. 35, n. Special, p. 955-968, 2020. DOI: http://dx.doi.org/10.1590/0102-7786355009. Available at: https://www.scielo.br/j/rbmet/a/j5XMWwf8tkZcw9nj94nXTPH/?format=pdf&lang=pt. Accessed on: March 2, 2021.

SILVA, AM; SILVA, RM; SILVA, BB Determination of surface temperature and estimation of net radiation and evapotranspiration using Landsat images and observed data. **Brazilian Journal of Cartography** , Rio de Janeiro, v. 67, n. 6, p. 1203-1216, 2015 .

SILVA, BBD; BRAGA, AC; BRAGA, CC; OLIVEIRA, L.M.; MONTENEGRO, SM; BARBOSA JUNIOR, B. Procedures for calculation of the albedo with OLI- Landsat 8 images : Application to the Brazilian semiarid . **Brazilian Journal of Agricultural and Environmental Engineering** , Campina Grande, v. 20, n. 1, p. 3-8, 2016.

SILVA, CVS; SILVA, JLB; MOURA, GBA; LOPES, PMO; NASCIMENTO, CR; SILVA, LC Remote sensing monitoring of vegetation cover in the Brazilian semiarid region using vegetation indices. **Nativa** , Sinop, v. 7, n. 6, p. 708-717, 2019. DOI: http://dx.doi.org/10.31413/nativa.v7i6.7646 . Available at : https://periodicoscientificos.ufmt.br/ojs/index.php/nativa/article/view/7646/6436. Accessed on: September 21, 2022.

SILVA; WTC; BARBOSA; HA Assessment of precipitation on sugarcane agricultural productivity: case study of the Coruripe mill for the 2000/2005 harvests. **Brazilian Journal of Physical Geography** , Recife, v. 15, n. 5, p. 2301-2312, 2021. DOI: https://doi.org/10.26848/rbgf.v14.3.p1352-1366. Available at: https://periodicos.ufpe.br/revistas/index.php/rbgfe/article/view/244967 . Accessed on: Aug. 14, 2022.

SIMÕES, EM; LIMA, JR; MENDONÇA, IFC Normalized difference vegetation index associated with rainfall variables for the Espinharas River subbasin – PB/RN. **Nativa** , Sinop, v. 9, n. 1, p. 106-114, 2021. DOI: https://doi.org/10.31413/nativa.v9i1.10453. Available at: https://periodicoscientificos.ufmt.br/ojs/ind ex.php/nativa/article/view/10453. Accessed on: September 20, 2022.

USGS. **Landsat 8 (L8) data users handbook** . Reston: USGS, 2016. Available at: earthexplorer.usgs.gov/. Accessed on: December 23, 2022.